A Hierarchical Multi-Parametric Programming Approach for Dynamic Risk-based Model Predictive Quality Control

Austin Braniff, Yuhe Tian*

Department of Chemical and Biomedical Engineering, West Virginia University, Morgantown, WV 26506, United States

Abstract

In this work, we present a hierarchical batch quality control strategy with real-time process safety management. It features a multi-time-scale framework augmenting: (i) Risk-aware model predictive controller for short-term set point tracking and dynamic risk control under disturbances; (ii) Control-aware optimizer for long-term quality and safety optimization over the entire batch operation; (iii) Intermediate surrogate model to bridge the gap by readjusting the optimizer operating decisions for the controller. All of the above problems are solved via multi-parametric mixed-integer quadratic programming with a key advantage to generate offline explicit control/optimization laws as affine functions of process and risk variables. This allows for the design of fit-for-purpose risk management plan prior to real-time implementationwhile reducing the need repetitive online dynamic optimization. A unified process model is used to underpin the consistency of hierarchical operational optimization. The proposed approach offers a flexible strategy to integrate distinct time scales which can be selected separately tailored to the process-specific need of control, fault prognosis, and end-batch quality control. A T2 batch reactor case study is presented to showcase this approach to systematically address the interactions and trade-offs of multiple decision layers toward improving process efficiency and safety.

Keywords: Quality Control, Multi-Parametric Model Predictive Control, Dynamic Risk Analysis, Multi-Time-Scale Optimization

1. Introduction

Chemical process operations typically follow a sequential and reactive strategy to determine process control and safety management actions based on set point deviations, product off-specifications, or fault occurrences at the current time step. It remains a central yet open research question on how to optimize operations integrally over multiple time scales to safely address the interactions and trade-offs between different tasks (e.g., control, real-time optimization, scheduling) [1, 2]. This work aims to investigate a representative process application requiring such multi-time-scale operational optimization [3, 4], i.e. the integration of batch process control, end-product quality control, and fault prognosis (as shown in Fig. 1).

In non-continuous processes (e.g., batch and semi-batch reactors), the end-product quality cannot be measured until the operation is terminated. It is thus essential to develop advanced control optimization techniques for real-time end-product quality prediction while optimizing process economics under disturbances [5, 6, 7]. An indicative list of research studies on batch quality monitoring and control is presented in Table

*Corresponding author at: Department of Chemical and Biomedical Engineering, West Virginia University, Morgantown, WV 26506, United States.

Email address: yuhe.tian@mail.wvu.edu (Yuhe Tian)

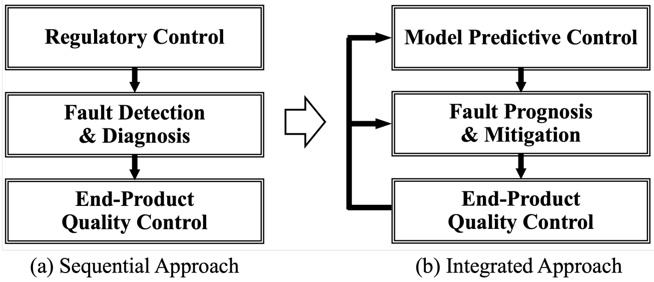

Figure 1: of process control, safety management, and quality assurance.

1. Theoretical approaches were developed using first principles model to quantitatively predict the entire batch trajectory [8, 9]. To circumvent process-specific model development, inferential quality monitoring was utilized in a corrective manner to adjust the batch operation path through predictions inferred by measured process data [10]. Online measured data could be analyzed via principal component analysis (PCA) or partial least-squares (PLS) regression [11, 12], coupled with data completion techniques to impute the "missing data" up to batch-end for quality estimation [13]. A more recent work [14] showed improved prediction accuracy using an augmented PLS model built on hybrid simulated and measured data. Data-driven batch monitoring approaches have received increasing interestwhich leverage support vector techniques and neural networks [15, 16]. For quality control, model predictive control (MPC) strategies have been further integrated with PCA and PLS modelswhich demonstrated superior performance than proportional-integral controllers [17, 18]. With advancements in real-time computing, nonlinear model predictive control (NMPC) was successfully applied to fed-batch bioreactors [19]. Similarly, economic model predictive control (EMPC) approaches can leverage modern computing power to solve batch control problems in an online fashion [20, 21]. Multi-parametric MPC (mp-MPC) provides an alternative strategy which can effectively enhance computational efficiency [22]. Explicit control laws can be generated offline a priori to replace online dynamic optimization with mp-MPC look-up map. Notably, the explicit solutions from multi-parametric programming also provide an instrumental link to integrate multi-time-scale (e.g., batch control and scheduling [23], simultaneous design and control [24]).

Process safety management presents an additional decision layer to prevent and minimize hazardous incidents due to, e.g.equipment failure. Extensive efforts have been made to integrate advanced control with fault diagnostic algorithms [26, 27], such as fault-tolerant control [28, 29] which takes reactive control actions to remedy fault from developing to severe failure. Fault prognosis [30, 31] has so far been under-exploited, which strives to detect fault at the early developing stage and predict its propagation to enable proactive risk management. Conventional process safety analyses (e.g., hazard and operability study [32, 33], quantitative risk assessment [34]) are performed prior to real-time operation and updated periodically throughout the plant lifetime such as every five years. However, they fail to capture the impact of dynamically varying operating conditions due to uncertainties or real-time [35]. Toward prognostic process safety management, model predictive safety system was developed to signal the alarm system if the plant model was foretasted to violate operability or safety constraints [36, 37]. Strategies to integrate process safety and control were proposed by characterizing a maximum set of the state space, within which the systems dynamic operation could be theoretically guaranteed as safe and stable, e.g.via pertinent systems theory [38] and Lyapunov level set [39]. The Lyapunov-based control approaches have also been extended to ensure stable and safe process operations from the aspect of [40]. Dynamic risk assessment offers another promising way forward for the online monitoring of process safety performance using timely-updated and process-specific probability and severity data [41, 42, 43]. Recent works explored the integration of dynamic risk assessment and model predictive control [44], leveraging the model-based moving horizon prediction for fault prognosis. Namely, if any fault is predicted during the next MPC output horizon, alarms would be triggered ahead of time. A major challenge to

Table 1: Batch quality monitoring and control approaches – an indicative list.

Focus	**Authors**	**Main Features**
Quality monitoring	Russell et al. [8]	Model-based state estimation framework to address uncertain initial conditions
	Nomikos & MacGregor [11]	Applying PCA and PLS to infer process variable trajectories
	Choi et al. [13]	Integrated methods with PCA and PLS
	Ghosh et al. [14]	Augmented PLS model built on hybrid simulated and measured data
	Yao et al. [15]	Data-driven approach based on functional support vector data description
	Kay et al. [16]	Soft sensor integrating autoencoder and heteroscedastic noise neural networks
Quality control	Kravaris et al. [9]	Nonlinear control algorithm for batch trajectory tracking
	Flores-Cerrillo & MacGregor [17]	Multivariate empirical model predictive control based on batch PCA models
	Mesbah et al. [25]	Dynamic control optimization based on nonlinear moment model
	Aumi et al. [18]	Integrating local data-driven models and inferential model for predictive control
	Chang et al. [19]	NMPC based on dynamic flux balance model for fed-batch reactors
	Rashid et al. [21]	EMPC approach for optimizing batch duration and economics

these approaches lies in the equivalence of controller output horizon with fault prognosis horizon. For process systems with very fast dynamic systems (e.g., seconds or less), the online MPC computational load will be intensive or even intractable to cover a 20-minute fault prognosis horizon which is essential for the operators to take responsive actions to alarms.

With the ongoing digital transformation creating more dynamic and interconnected chemical plants, a systematic approach is essential yet currently lacking which can fully integrate process control, end-batch quality control, and fault prognosis to increase the overall process efficiency under uncertainties with guaranteed process safety. To address this gap, this work proposes a hierarchical risk-based model predictive quality control approach which augments multiple multi-parametric problems to bridge the large time span in a temporally scalable manner. The remaining sections of this paper are structured as follows: Section 2 introduces the proposed approach for risk-based model predictive quality control with hierarchical multi-parametric optimization formulations, particularly highlighting the role of explicit solutions. Section 3 demonstrates the approach on a case study of safety-critical batch reactor. Section 4 presents concluding remarks and ongoing work.

2. Methodology: Risk-based Model Predictive Quality Control

In this section, we first provide an overview of the proposed methodology followed by the detailed mathematical modeling and formulation of each supporting component.

2.1. Overview of the Methodology

The proposed hierarchical approach for risk-based model predictive quality control is shown in Fig. 2, which integrates the following key components:

- *Short-term risk-aware controller* — which determines the optimal control actions on a characteristically short (e.g., minutes or seconds). The controller is designed for dynamic risk monitoring and control for safety considerations [45, 46] in addition to performing routine tasks such as disturbance rejection and set point tracking of major process variables (e.g., temperature, purity).

- *Long-term control-aware safety and quality optimizer* — which delivers an optimal input/output set point trajectory over a characteristically long . The optimizer forecasts the entire (or sufficiently long) batch duration, ensuring operational safety and quality targets to be satisfied. The input/output set

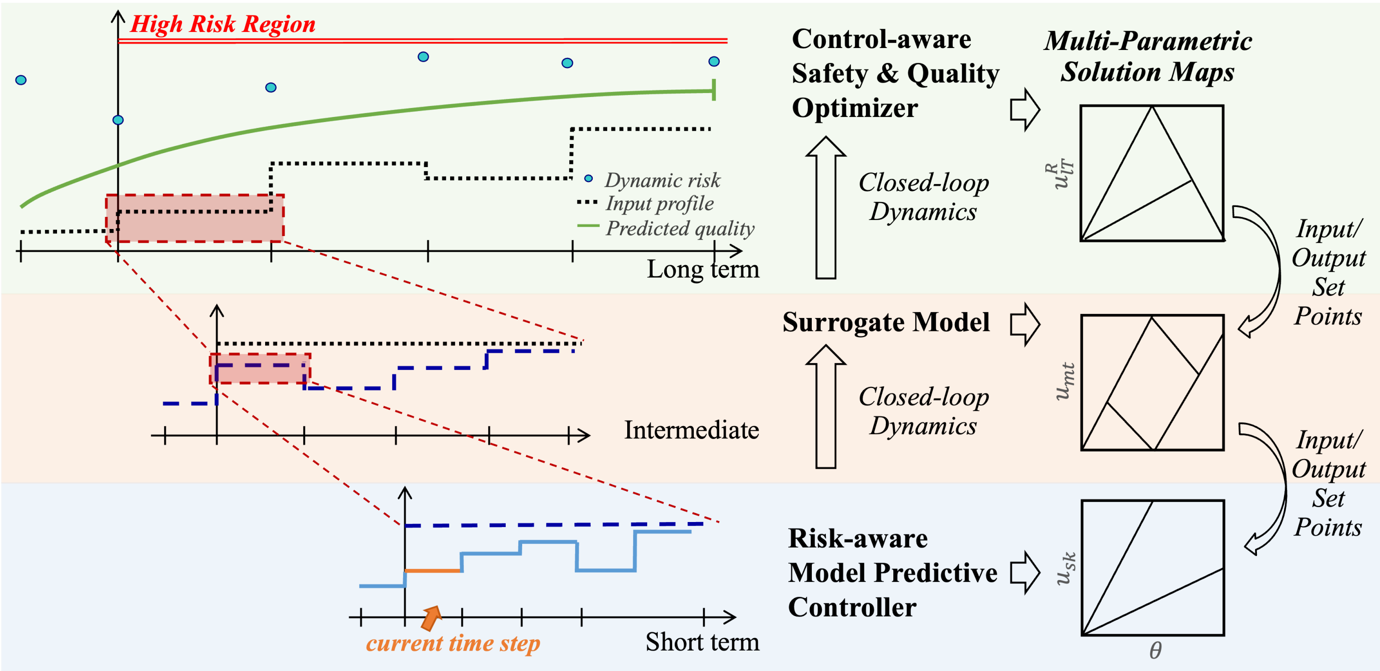

Figure 2: Hierarchical risk-based model predictive quality control.

points are used to guide the controller operations. Economics considerations can also be included in the optimizer objective function.

- *Intermediate surrogate model* – which aims to mitigate the optimizer and controller discrepancy. When necessary, the surrogate model [23] translates the optimizer decisions at a larger time step to more achievable set points for the controller at a smaller time step.

The risk controller, quality optimizer, and surrogate model are built on the same process and safety system model to ensure consistency. It is worth highlighting that the optimizer and surrogate model utilize the closed-loop form of process and safety system model, thus being aware of the risk control actions in a predictive manner. All these three-level decision makers are solved as multi-parametric (mixed-integer) linear/quadratic programming problems, from which explicit solution maps can be obtained offline a priori. A general multi-parametric quadratic programming (mp-QP) problem is given in Eq. 1 to showcase the idea of explicit solutions. More detail can be found in the recent books [22, 47]. As such, the online implementation only requires affine function evaluation using the explicit solution maps instead of repetitively performing online dynamic optimization.

Example of mp-QP and explicit solutions

$$
\begin{aligned}
J^*(\theta) \quad &= \min_z \tfrac{1}{2} z^T Q z + c^T z \\
\text{s.t.} \qquad Az \quad &\leq b + F\theta \qquad\qquad (1)\\
A_{eq}z \quad &= b_{eq} + F_{eq}\theta
\end{aligned}
$$

where z is the vector of decision variables, θ is the vector of uncertain parameters which can include state variables, set points, disturbances, etc. in process control applications, A and b are the coefficient matrices to define the inequality constraints, A_{eq} and b_{eq} are the coefficient matrices to define the equality constraints. The optimal decision variables z^* can be explicitly expressed as a function of the uncertain parametersθas presented in Eq. 2. Key theoretical properties of the explicit solutions include: (i) $z^*(\theta)$ is continuous and piece-wise affine, (ii) the uncertain parameter space is partitioned to convex polyhedral regions (i.e., critical regions CR), and (iii) the optimal objective function $J^*(\theta)$ is convex and piece-wise quadratic.

$$z^*(\theta) = \begin{cases} K_1\theta + r_1, \theta_1 \in CR^1 = \{CR^1_A\theta_1 \leq CR^1_b\} \\ \vdots \\ K_i\theta + r_i, \theta_i \in CR^i = \{CR^i_A\theta_i \leq CR^i_b\} \end{cases} \tag{2}$$

where K and r are coefficient matrices to define the explicit solutions, CR^A and CR^b are coefficient matrices to define the corresponding critical regions.

2.2. Modeling and Hierarchical Multi-parametric Formulations

Hereafter, we discuss each key element constituting the above risk-basemodel predictive control approach.

2.2.1. Dynamic Risk Modeling

Dynamic risk modeling by Bao et al. [45] is adopted to indicate online process safety performance based on the real-time values of safety-critical process variables (e.g., x_t). Some of its key features to enable the integration with process control and real-time include: (i) The support of real-time process safety monitoring by updating fault probability and severity consequence in an instant manner as a function of safety-critical process variables, (ii) $P(x(t))$ and $S(x(t))$ take standardized values at $\mu \pm 3\sigma$, which provide a uniform basis to compare the safety performance of different process operating strategies, (iii) Model-based forecast can be implemented, as showcased in this work, leveraging the MPC and operational optimization formulations. As shown in Eq. 3a, the dynamic risk index $RI(t)$ is defined as the product of fault probability $P(t)$ and consequence severity $S(t)$. This work assumes that x_t follows the Gaussian probability distribution with the mean as μ (i.e., nominal operating condition) and the standard deviation as σ. Based on statistics, 99.7% of the x_t values are expected to fall within the three-sigma region (i.e., three-sigma rule). $\mu \pm 3\sigma$ is therefore utilized as the upper and lower control limit. The high risk region is defined as RI value greater than a certain threshold. The threshold value is determined based on prior process knowledge and/or historical operating data, beyond which the process is at a higher probability of abnormal operations. The fault probability $P(t)$ is calculated via the Gaussian probability density functionas shown in Eq. 3b. The fault probability is thus standardized at $\mu \pm 3\sigma$, which provides a normalized benchmark enabling the comparison of different process operation (and design) strategies against process safety considerations [48]. The consequence severity $S(t)$ is calculated using an exponential function based on the deviation of $x(t)$ from the nominal operating condition, as given in Eq. 3c.

As a result, the overall risk index $RI(t)$ emerges as a nonlinear pseudo-exponential function as shown in Fig. 3a, which grows increasingly faster as x_t departs from the nominal operating conditions. The formulation of Eq. 3 renders a notably higher risk when x_t falls out of the three-sigma region (i.e., when the 0.3% low probability events happen). This feature is instrumental for the integration of real-time process safety management with process operations, as it allows the controller and optimizer to systematically decide the priority among various operational objectives. For example, if the risk index is high or predicted to escalate, the controller and optimizer will prioritize risk mitigation. In contrast, if the risk index is relatively low, the controller and optimizer will prioritize to optimize operational stability, costs, and/or end-batch quality. A piece-wise linearization formulation (Eq. 4) is further developed to approximate the original pseudo-exponential formulation as shown in Fig. 3b. In the cases when the critical process variables follow more nonlinear distributions, e.g.binomial distributions, the piece-wise linearization can be conducted in a generalized manner to approximate the original function. This allows for a linear model-based control scheme which will be discussed in the next section. Although a linear form of the dynamic risk model is to be used for control, the original nonlinear nature of the risk model is critical. This is because the nonlinear risk model dictates the different operating regions according to risk propagation speeds, which is further reflected by the piece-wise linearization. Therefore, the process and risk control can be self-adaptive to different operational objectives, e.g.to sustain stable operation or to adapt increasingly aggressive risk control.

Original formulation

$$RI(t) = P(t) \times S(t) \tag{3a}$$

$$P(x_t) = \int_{-\infty}^{x_t} \frac{1}{\sqrt{2\pi}\sigma} e^{-\frac{[x_t-(\mu\pm3\sigma)]^2}{2\sigma^2}} dt \tag{3b}$$

$$S(x_t) = 100^{\frac{(\mu\pm3\sigma)-x_t}{\mu-x_t}} \tag{3c}$$

Piece-wise linearization

$$RI(t) = \begin{cases} m_1 x(t) + b_1, & x(t) \in [\,\underline{x}_1, \overline{x}_1\,) \\ m_2 x(t) + b_2, & x(t) \in [\,\underline{x}_2, \overline{x}_2\,) \\ m_3 x(t) + b_3, & x(t) \in [\,\underline{x}_3, \overline{x}_3\,) \\ m_4 x(t) + b_4, & x(t) \in [\,\underline{x}_4, \overline{x}_4\,] \end{cases} \tag{4}$$

where m and b are the slope and intercept of the piece-wise linearized risk functions, underbar and overbar respectively represent the lower and upper bounds for a given parameter, and subscript $i \in \{1, 2, 3, 4, ...\}$ denotes the corresponding linearized region as illustrated in Fig. 3b.

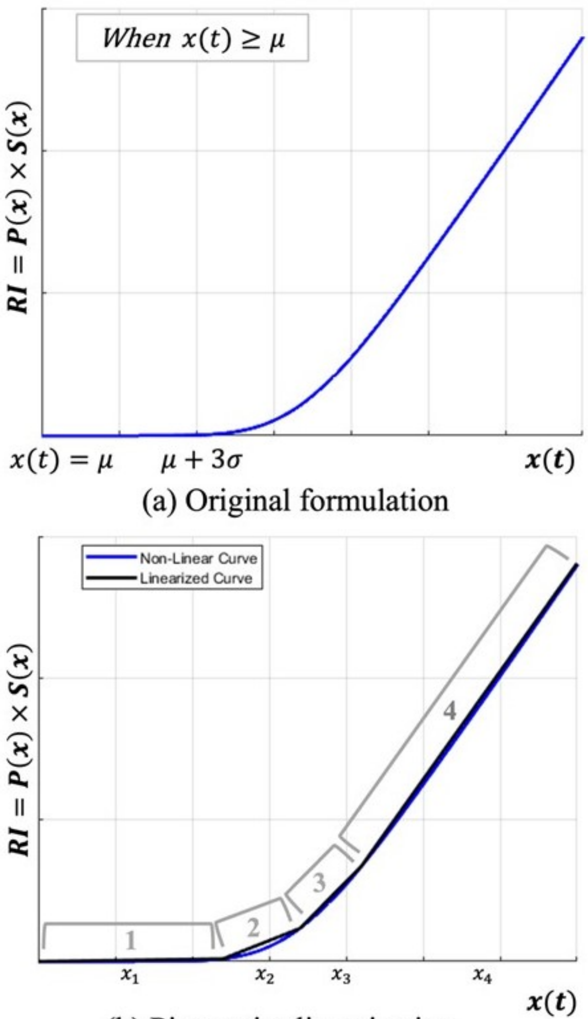

(a) Original formulation

(b) Piece-wise linearization

Figure 3: Dynamic risk modeling

2.2.2. Short-Term Risk-Aware Controller

Based on the above dynamic risk model, a risk-aware model predictive control strategy has been developed in our prior work [46]. For the continuity of this work, the MPC formulation is briefly introduced in what follows using Eq. 5. The control objective (Eq. 5a) can be defined for set point tracking, disturbance rejection, etc. The risk index can also be treated as an output variable and incorporated into the control objective, as will be showcased later in this work. Eqs. 5b-c present the linearized process state space model which can be obtained from nonlinear high-fidelity process models using Jacobian linearization [49], model approximation [24, 50], or data-driven modeling [51, 52]. Eqs. 5d-f reformulate the piece-wise dynamic risk model (Eq. 4) using mixed-integer linear equations. j_i is introduced as a binary variable to denote if the current safety-critical variable $x(t)$ lies in the i^{th} linearized region (or not), thereby activating the corresponding RI linear approximation (or not). For example, if the $x(t)$ lies in the first section ($x_{1,lo} \leq x \leq x_{1,up}$), then Eq. 5f holds true with $j_1 = 1, j_2, j_3, j_4 = 0$. As a result, Eq. 5e gives $M = m_1$ and $b = b_1$ which renders Eq. 5d to be $RI - b_1 = m_1 x$. This approach thus ensures that the slope (M) and y-intercept (b) in Eq. 5d are the slope and y-intercept of the active section of the linearized Risk Index in Eq. 4. In this way, the optimal risk control decisions are made based on the combined process and risk model, which is crucial for the systems-based operations and safety-critical to be aware of each other. Eqs. 5g-h include path constraints to state, input, output, and risk variables. Therefore, this risk-aware MPC strategy offers two layers of process safety management: (i) Control of dynamic risk as an overarching operational objective, (ii) Constraining the operating path within a safe state space. Eq. 5 can be reformulated into a multi-parametric mixed-integer quadratic programming (mp-MIQP) problem [46]. As the binary variables j_i are mutually exclusive (Eq. 5f), the mp-MIQP problem can be simplified to a number of mp-QP problems valid at the corresponding linearized risk region. Explicit risk-aware control laws can be obtained as piece-wise affine functions of states, outputs, risk index, set points, and disturbances (Eq. 6).

Explicit control laws and critical regions

$$\begin{aligned}\min_{u_{sk}} \quad & x_N^T P x_N + \sum_{t=1}^{OH-1} (y_{sk} - y_{sk}^R)^T QR_k (y_{sk} - y_{sk}^R) \\ & + \sum_{t=0}^{CH-1} (u_{sk} - u_{sk}^R)^T R_k (u_{sk} - u_{sk}^R)\end{aligned} \tag{5a}$$

$$\text{s.t.} \quad x_{sk+1} = A_s x_{sk} + B_s u_{sk} \tag{5b}$$

$$y_{sk} = C_s x_{sk} + D_s u_{sk} \tag{5c}$$

$$RI_{sk} - b = M x_{sk} \tag{5d}$$

$$\sum_i m_i j_i = M \quad \sum_i b_i j_i = b \quad \sum_i x_i j_i = x_{sk} \tag{5e}$$

$$\sum_i j_i = 1 \quad j_i \in \{0,1\} \quad x_{i,lo} j_i \le x_i \le x_{i,up} j_i \tag{5f}$$

$$\underline{x}_{sk} \le x_{sk} \le \overline{x}_{sk} \qquad \underline{u}_{sk} \le u_{sk} \le \overline{u}_{sk} \tag{5g}$$

$$\underline{y}_{sk} \le y_{sk} \le \overline{y}_{sk} \quad \underline{RI}_{sk} \le RI_{sk} \le \overline{RI}_{sk} \tag{5h}$$

where subscript sk denotes the short time step for risk-aware control, i represents the different regions of the linearized risk model. P is terminal weight, QR and R are controller weights, CH and OH are respectively control and output horizons, x is the vector of state variables, y is the vector of output variables, u is the vector of input variables, d is the vector of disturbances, A_s, B_s, C_s, and D_s are matrices of the linearized state space model. Superscript R defines set point.

Explicit risk-aware control laws

$$\begin{aligned} u_{sk} &= K_{i,sk}\theta_{sk} + r_{i,sk} \\ \theta_{sk} \in CR^i &= \{CR^i_{A,sk}\theta_{sk} \le CR^i_{b,sk}\} \\ \theta_{sk} &= [x_{sk}, y_{sk}, RI_{sk}, y_{sk}^R, d_{sk}] \end{aligned} \tag{6}$$

where θ defines the parameter set for mp-MPC, CR are critical regions. CR_A and CR_b are coefficient matrices for critical regions.

2.2.3. Long-Term Control-Aware Safety and Quality Optimizer

The optimizer contributes to maintain an acceptable level of risk for the process while reaching end-batch quality specifications. It forecasts and optimizes the process safety, quality, and/or economics performance over a sufficiently long time span, ideally up to the end of batch. The mathematical formulation of this optimization problem is presented in Eq. 7. The objective function (Eq. 7a) can be formulated in linear or quadratic form accounting for the minimization of cost, energy consumption, and/or offsets from quality target, etc. The optimizer utilizes the closed-loop process and safety state space model (Eqs. 7b-c), i.e. with the risk-aware control laws integrated. A larger time step lT is adopted to ensure the computational efficiency for prediction over hours or even days. This safety and quality optimizer problem is also reformulated into mp-MIQP problems, generating explicit solutions prior to online operationas given in Eq. 8. The resulting input, output, and/or risk set points (u_{lT}^R, y_{lT}^R, RI_{lT}^R) are then sent to guide the operations of the risk-aware controller. The optimizer provides key advantages which include:

- Enhanced computational efficiency and prediction accuracy – as the methodology avoids relying on the risk-aware controller for end-batch quality prediction which may require a significantly large number of output horizons at smaller control time steps.

- Flexible selection of controller and optimizer time scales – while their fully integrated, the selection of respective time scales is independent. This leads to a temporally scalable methodology to fit the purpose of distinct operational optimization objectives across multiple time scales (e.g., short-term control versus long-term cost optimization).

- Prescriptive safety management – The optimizer adds another layer of dynamic risk forecast and fault prognosis over a longer time horizon, particularly assessing the impact on safety of real-time operational decisions under disturbances.

Optimizer formulation

$$\min_{u^R_{lT}} \quad \sum W_1||y^R_{lT} - y^{QT}||^{p_1} + W_2||y^R_{lT}||^{p_2} + W_3||u^R_{lT}||^{p_3} \tag{7a}$$

$$\text{s.t.} \quad x_{lT+1} = A_l x_{lT} + B_l u^R_{lT} + C_l d_{lT} \tag{7b}$$

$$\begin{bmatrix} y^R_{lT} \\ RI^R_{lT} - b \end{bmatrix} = \begin{bmatrix} D_l \\ M_l \end{bmatrix} x_{lT} + \begin{bmatrix} E_l \\ 0 \end{bmatrix} u^R_{lT} \tag{7c}$$

$$\underline{x}_{lT} \leq x_{lT} \leq \overline{x}_{lT} \qquad \underline{u}^R_{lT} \leq u^R_{lT} \leq \overline{u}^R_{lT} \tag{7d}$$

$$\underline{y}^R_{lT} \leq y^R_{lT} \leq \overline{y}^R_{lT} \qquad \underline{RI}^R_{lT} \leq RI^R_{lT} \leq \overline{RI}^R_{lT} \tag{7e}$$

where subscript lT denotes the long time step for control-aware optimizer, W_1 and W_2 are weighting matrices for quality and input-related economics considerations, p_1, p_2, p_3 can take the value of 1 or 2 resulting in linear or quadratic objective functions, y^{QT} are the quality control targets, and the matrices of the state space model A_l, B_l, C_l, D_l, and E_l are derived by first simulating closed-loop input-output data with risk controller on and employing system identification techniques.

Explicit control-aware optimizer solutions

$$\begin{aligned} u^R_{lT} &= K_{i,lT}\theta_{lT} + r_{i,lT} \\ \theta_{lT} \in CR^i_{lT} &= \{CR^i_{A,lT}\theta \leq CR^i_{b,lT}\} \\ \theta_{lT} &= [x_{lT}, y^R_{lT}, RI^R_{lT}, y^{QT}_{lT}, d_{lT}] \end{aligned} \tag{8}$$

2.2.4. Intermediate Surrogate Model

For substantially different time scales, it may be possible that the operating path suggested by the optimizer misses important process and safety dynamics or constraints such that the long-term set points are not achievable or overly aggressive to the risk-aware controller. In this instance, it becomes essential to interpret the input/output set points from the optimizer for the risk-aware controller using an intermediate to ensure smooth operational transitions while still reaching the end-point quality with desired process safety performance. To this purpose, a surrogate modeling approach [23] is employed as shown in Eq. 9. The quality control performance will be the first criterion if an intermediate surrogate model should be applied. If desired quality control performance can be achieved, an intermediate surrogate model may not be necessary. Otherwise, if off-spec behavior is observed as that shown in Fig. 11, some important process dynamics may be missed due to the lack of an intermediate surrogate model. Computational load presents another main reason for having a surrogate model, in order to cover longer optimizer predictions but with a tractable number of time steps. The surrogate model aims to determine the new set points at the intermediate time step (mt) by minimizing their squared error against the optimizer set points at longer time steps (lT). This intermediate sampling interval is currently determined via trial-and-error tuning to obtain desired control performance. There exists a tradeoff where smaller intervals can better capture the system dynamics, but the set points from the long term optimizer may be too aggressive to be achieved during the small time duration. On the other hand, larger intervals face the risk of missing certain important system dynamics (e.g., change of process gain) while may also provide smoother transition between the long-term optimizer and short-term controller. As shown in Eq. 9, the surrogate model is also built on the closed-loop process and safety state space model, i.e. with the risk-aware control laws integrated. The state-space model in Eqs. 9b-c can be obtained via two strategies: (i) re-discretizing Eqs. 7b-c to smaller time steps, or (ii) re-performing systems identification using input-output closed loop control data with risk-aware controller active. The surrogate model is again formulated as an mp-MIQP problem with the mixed-integer variables resulted from piece-wise risk linearization. The explicit solutions are exemplified in Eq. 10 for the model-based mapping between the surrogate model set points and optimizer set points.

Surrogate model formulation

$$\min_{u^R_{mt}} \quad \sum ||y^R_{mt} - y^R_{lT}||^2 + ||u^R_{mt} - u^R_{lT}||^2 \tag{9a}$$

$$\text{s.t.} \quad x_{mt+1} = A_m x_{mt} + B_m u^R_{mt} + C_m d_{mt} \tag{9b}$$

$$\begin{bmatrix} y^R_{mt} \\ RI^R_{mt} - b \end{bmatrix} = \begin{bmatrix} D_m \\ M_m \end{bmatrix} x_{mt} + \begin{bmatrix} E_m \\ 0 \end{bmatrix} u^R_{mt} \tag{9c}$$

$$\underline{x}_{mt} \leq x_{mt} \leq \overline{x}_{mt} \qquad \underline{u}^R_{mt} \leq u^R_{mt} \leq \overline{u}^R_{mt} \tag{9d}$$

$$\underline{y}^R_{mt} \leq y^R_{mt} \leq \overline{y}^R_{mt} \quad \underline{RI}^R_{mt} \leq RI^R_{mt} \leq \overline{RI}^R_{mt} \tag{9e}$$

where subscript mt refers to the intermediate time step of the surrogate model.

<u>*Explicit surrogate model solutions*</u>

$$\begin{aligned} u^R_{mt} &= K_{i,mt}\theta_{mt} + r_{i,mt} \\ \theta_{mt} \in CR^i_{mt} &= \{CR^i_{A,mt}\theta \leq CR^i_{A,mt}\} \\ \theta_{mt} &= [x_{mt}, y^R_{mt}, RI^R_{mt}, y^R_{lT}, RI^R_{lT}, u^R_{lT}, d_{mt}] \end{aligned} \tag{10}$$

2.3. Remarks

For the introduced risk-based model predictive quality control approach, three explicit/multi-parametric solution maps are respectively obtained for the hierarchical control-aware safety and quality optimizer, intermediate surrogate model, and risk-aware controller. In this way, the decisions from upper-level (in longer term) can be seamlessly conveyed to the lower-level (in shorter term), while the lower-level dynamics are explicitly aware by the long-term representation. Several remarks can be made here to highlight the key advantages of this proposed approach: (i) Multi-parametric programming enables the generation of explicit control or optimization solutions a priori as piece-wise affine functions of process states, outputs, risk, disturbances, etc. From this, a quantitative and algorithmic understanding on the impact of disturbances and real-time (e.g., set point selection) can be generated even before operating the process online. The risk controller can thus be tuned accordingly to maximize the safe operating region against disturbances, while simultaneously optimizing the overall batch efficiency and productivity; (ii) Different operating tasks (e.g., control, cost, fault prognosis) can exhibit distinct slower or faster dynamical time scales spanning from seconds to hours. The three-level hierarchical formulation addresses the respective tasks at their characteristic time scales while effectively integrating the at a supervisory level instead of undertaking all the decisions at every minimum time step; (iii) Multi-parametric programming replaces repetitive online optimization with online affine function evaluation, which has been proven to significantly reduce online computational time and computing resources. Tackling such multi-time-scale optimization using classic MPC typically results in a large scale mixed-integer dynamic optimization problem which is inefficient or computationally intractable.

When necessary, an online (mixed integer) dynamic optimization problem can be further posed to optimize process economics, energy efficiency, sustainability, etc. by coordinating the optimizer, surrogate model, and controllers together. As shown in Eq. 11, this approach provides an instrumental feature to utilize a single online dynamic optimization problem while addressing additional needs beyond quality control, such as response to demand changes. This optimization problem features: an objective function, the nonlinear process model, the nonlinear risk model, explicit controller solutions, explicit optimizer solutions, explicit surrogate model solutions, and path constraints. The ability to utilize the high fidelity process and risk models in online optimization is also critical to close the loop with the original nonlinear process systems. The current work leverages the hierarchical approach to extend the safety and quality optimizer to cover a significantly longer horizon than the risk controller. However, the methodology generally intends to decompose the operational optimization complexity for any systems with intrinsic disparate dynamics (e.g., fast, slow, and/or hybrid). In addition, the current work assumes that a verified high fidelity process model is available for model-based control optimization. The extension to (physics-guided) data-driven modeling and online model updating using real-time measurement data can be referred to our recent work [51, 53].

$$\begin{aligned} min \quad & F = \textstyle\int_0^\tau P(x(t), y(t), RI(t), u(t), d(t))dt \\ \text{s.t.} \quad & dx(t)/dt = f(x(t), u(t), d(t)) \\ & RI = RI(x(t), u(t), d(t)) \\ & u_{sk} = K_{i,sk}\theta_{sk} + r_{i,sk} \\ & u^R_{lT} = K_{i,lT}\theta_{lT} + r_{i,lT} \\ & u^R_{mt} = K_{i,mt}\theta_{mt} + r_{i,mt} \\ & \underline{x} \leq x(t) \leq \overline{x}, \quad \underline{u} \leq u(t) \leq \overline{u} \\ & \underline{y} \leq y(t) \leq \overline{y} \qquad \underline{RI} \leq RI(t) \leq \overline{RI} \end{aligned} \tag{11}$$

3. Case Study – Safety-Critical T2 Batch Reactor

In this section, we apply the above methodology on a safety-critical exothermic batch reactor. This case study is conceptualized from the batch production process at T2 Laboratories Inc., which suffered from a process safety incident in 2007 resulting in four deaths and twenty-eight injuries [54]. Various application scenarios are investigated to demonstrate the potential, efficacy, and flexibility of the proposed method to integrate process control, dynamic risk management, and end-batch quality control.

3.1. Process Description

A schematic of this T2 batch reactor is shown in Fig. 4. It has two feed streams respectively including methylcyclopentadiene (A), sodium (B), and diglyme (S) to produce sodium methylcylcopentadiene (C) as a desired product for gasoline additive and hydrogen (D) as a side product. The two exothermic reactions occurring in this reactor are given below. The activation energy of the side reaction is substantially larger than the main reaction, which makes the side reaction rate only significant at elevated temperatures. However, if cooling utility is not adequately suppliedin the 2007 incident, the batch reactor temperature may increase uncontrollably which will eventually ignite the hydrogen and lead to explosion.

<u>Main reaction:</u>

$$\text{Methylcyclopentadiene (A)} + \text{Sodium (B)} \xrightarrow{Diglyme(S)} \text{Sodium Methylcyclopentadiene (C)} + \text{Hydrogen (D)}$$

<u>Side reaction:</u>

$$\text{Diglyme (S)} \xrightarrow{Sodium(B)} \text{Hydrogen (D)} + \text{Byproduct}$$

The research objective of this study is to determine the optimal batch operating strategy which can:

- Meet the end-batch product quality target which is defined against the conversion of raw material A.
- Provide safe and optimal operations under disturbances, ideally operating at the low risk level throughout batch duration.

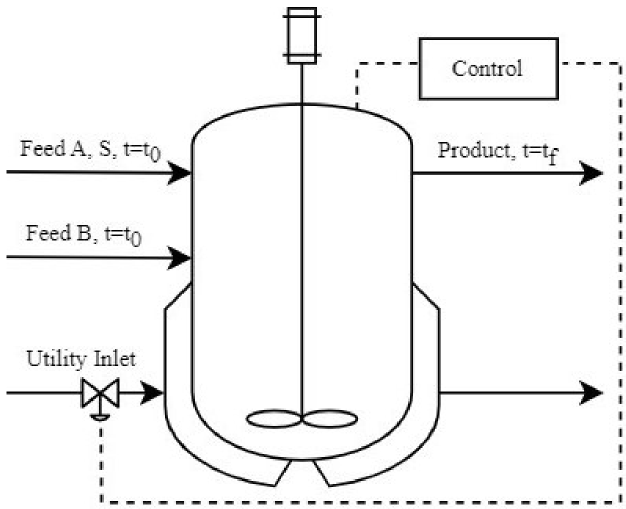

Figure 4: T2 batch reactor diagram

- Prevent the process from entering the high risk region. However, if fault occurrence cannot be circumvented, raise alarm ahead of time to allow the operators to prudently plan for emergency shutdown.

3.2. Process and Risk Modeling

A first principles model is developed to describe this reactoras given in Eq. 12. More specifically, Eqs. 12a-c define component mass balances and Eq. 12d calculates energy balance. The major process variables and parameters are summarized in Table 2. The current work assumes that the above model provides an accurate description for this batch reactor and mainly focuses on the development of a hierarchical risk-based quality control strategy. To improve the accuracy of the simulated model in real-world industrial applications, online model approximation can be adopted using real-time measurement data. An approach to this, as outlined in our prior work [53], is to use physics-informed machine learning techniques to estimate parameters in Eq. 12 based on plant data. System identification and machine learning approaches can also be directly utilized to obtain state space models from plant data, which can then be used to construct the risk control algorithms [55, 51].

$$\frac{dC_A}{dt} = -k_1 C_A C_B \tag{12a}$$

$$\frac{dC_B}{dt} = -k_1 C_A C_B \tag{12b}$$

$$\frac{dC_S}{dt} = -k_2 C_S \tag{12c}$$

$$\frac{dT}{dt} = \frac{V\sum(-\Delta H_k r_k) - UA_x(T - T_c)}{C_P \sum N_i} \tag{12d}$$

As shown in Fig. 4, the valve opening for the cooling utility stream is used in practice for reactor temperature control. For the simplicity of process modeling in this work, the heat transfer coefficient U is utilized as the manipulated variable which is proportional to the utility flow rate. This case study allows for cooling through negative U values which is essential for process safety management, while also enabling heating through positive U values to accelerate reactant conversions and meet quality targets. It is recognized that this represents a simplified modeling consideration, while in practice this may require a more complicated control system design to achieve the cease of flow for one utility and the emergence of flow for the other.

The dynamic risk model is then developed in accordance with Eq. 3. Based on literature [38], the nominal reactor operation temperature is selected as 460 K. When temperature exceeds 480.34 K, the reactor has a higher probability for thermal runaway. Therefore, the risk index is defined as a function of temperature which is the key safety-critical variable in the process. The mean (μ) is adopted as 460 K with a standard deviation (δ) of 5 K, which results in the upper control limit as 475 K (i.e., $\mu+3\delta$). In practice, the values of mean and standard deviation are determined by the engineers based on prior process knowledge and operating data. As shown previously in Fig 3, the risk index begins to rapidly increase when the process is 3δ away from the mean value μ. Specifically for this case study, the value of the risk index becomes significant at 475 K for the controller to take actions which gives a 5 K buffer region from entering the high risk region over 480.34 K (equivalently, $RI \geq 3$).

3.3. Risk-Aware Model Predictive Control

A combined linearized process and risk model is developed for its use in model predictive control. A discrete state space model is obtained from the batch reactor nonlinear first principles model (Eq. 12) using the MATLAB® system identification toolbox [56]. The time step is selected as 5 minutes due to the slow dynamics of this reactor. Note that the physical meanings of state variables ($\overline{x}$) are not retained in the identified state space model. Thus it is necessary to estimate the states of the system based on measured outputs which assumes an accurate online output measurement of temperature. The Jacobian method provides an alternative model linearization strategy [46]. However, to ensure sufficient model accuracy, successive online model linearization is found to be necessary for batch processes due to the lack of steady states. An additional case-study on risk-aware control utilizing the Jacobian method to derive state-space models of the system is provided in the Supporting Information. The implementation shows that the Jacobian requires excessive updates as the batch system is intrinsically dynamic. For each new Jacobian, new multi-parametric model predictive control (mp-MPC) laws should be generated via online computation. This would no longer leverage the advantage of mp-MPC to obtain explicit control laws offline a priori and to reduce online computational loads. This is why system identification is adopted in this work which can provide a single linearized batch model with sufficient modeling accuracy. The nonlinear dynamic risk model is also reformulated into disjoint piece-wise affine functions. The risk model is integrated with the process state space model by treating RI as an output and appending the necessary relationships with state variablesas presented in Eq. 13.

$$\overline{x}_{sk+1} = A\overline{x}_{sk} + BU_{sk} \tag{13a}$$

$$RI_{sk} - b = M\overline{x}_{sk} \tag{13b}$$

The coefficient matrices A, B, M, and linearization parameters m and b are given below. m and b are to be recast as mixed-integer expressions following Eqs. 5d-f.

$$\begin{aligned} A &= \begin{bmatrix} 1.0088 & -0.0495 \\ 0.1008 & 0.4611 \end{bmatrix} \\ B &= \begin{bmatrix} -1.520 \times 10^{-7} \\ -1.945 \times 10^{-6} \end{bmatrix} \\ M &= m \begin{bmatrix} -1.017 \times 10^{3} \\ 8.250 \times 10^{1} \end{bmatrix}^T \end{aligned} \tag{14}$$

Table 2: List of major batch process variables and parameters.

State variables	C_A, C_B, C_S: Concentrations, T: Temperature
Manipulated variable	U: Heat transfer coefficient
Control variable	RI: Risk
Disturbance	T_0: Initial Temperature
Model parameters	V: Volume (4000 L), ρ: Mixture density (36 mol/L) C_p: Specific heat (430.91 J/mol·K) A_x: Heat transfer area (5.3 m^2), T_c: Coolant (373K) ΔH_k:Heat of reaction (-45.6 kJ/mol, -320 kJ/mol) $k_i = A_i \exp(-\frac{E_i}{RT})$: Reaction rate constant for reaction i A_i: Frequency factor ($A_1 = 4 \times 10^{14}$, $A_2 = 1 \times 10^{84}$) E_i: Activation energy ($E_1 = 1.28 \times 10^5$, $E_2 = 8 \times 10^5$ J/mol·K)

$$m = \begin{cases} 0.00776, & T \in [460, 472] \\ 0.21471, & T \in (472, 477] \\ 0.54957, & T \in (477, 481] \\ 0.76287, & T \in (481, 495] \end{cases}$$
$$b = \begin{cases} -3.5717, & T \in [460, 472] \\ -101.25, & T \in (472, 477] \\ -260.98, & T \in (477, 481] \\ -363.58, & T \in (481, 495] \end{cases} \tag{15}$$

A risk-aware MPC problem is then developed as per Eq. 5 to optimally manipulate the heat transfer coefficient (U) to keep the risk index (RI) at the desired low risk level ($RI_{sk}^R = 0$). The tuning parameters and path constraints for the risk-aware control are summarized in Tables 3 and 4.

Table 3: Risk-aware controller – Tuning parameters

QR_k	R_k	OH	CH
1×10^8	1×10^{-6}	3	1

Table 4: Risk-aware controller – Path constraints

	U	RI	$\overline{x}_1, \overline{x}_2$
Min	-5.5×10^4	-3	$-100, -100$
Max	5.5×10^4	25	$100, \quad 100$

The risk-aware control problem is solved via mixed-integer quadratic programming to generate explicit control solutions. The closed-loop risk control performance is showcased in Figs. 5 and 6, which respectively present the scenario with initial conditions at a low risk level ($RI = 0$ equivalent to $T = 460K$) and a moderate risk level ($RI = 0.062$ equivalent to $T = 468K$). It is worth highlighting that, despite the explicit control laws are designed based on the linearized model, the closed-loop control and operational optimization throughout this work are implemented against the original nonlinear process model given in Eqs. 12a-d. In both scenarios, the risk-aware controller is able to eventually stabilize the process at the desired risk set point ($RI_{sk}^R = 0$). With a low-risk initial condition (Fig. 5), the controller succeeds in maintaining $RI \approx 0$ throughout the operations. With a moderate-risk initial condition (Fig. 6), a slight risk increase is observed while it is controlled back to the set point shortly after. Without the risk-aware control, it is shown that this process quickly reaches the high risk region.

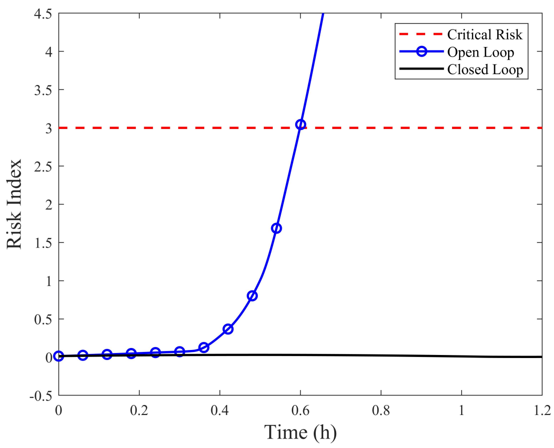

Figure 5: Open-loop and closed-loop simulation – Low risk initial condition.

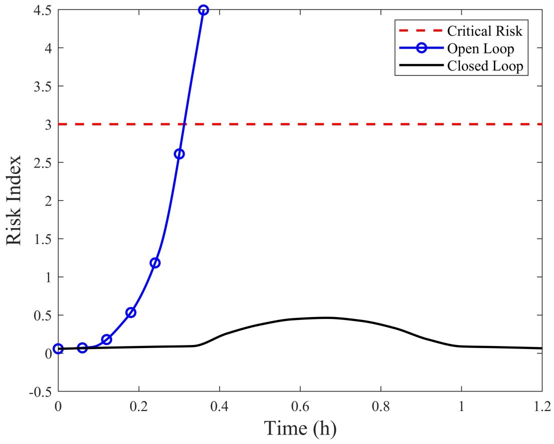

Figure 6: Open-loop and closed-loop simulation – Moderate risk initial condition.

3.4. Integration with Safety and Quality Optimization

The long-term safety and quality optimizer determines the optimal set points for the risk controller or surrogate model at a supervisory level by forecasting the operations throughout the batch. It also employs a linearized discrete state-space model which is developed using the MATLAB® system identification toolbox [56]. As the states of the linearized state space model become physically meaningless due to system identification (Eq. 13a), they should be estimated utilizing online output measurements which in this scenario is the temperature and the concentration of species A, i.e. C_A. In practice, if the concentration is not measurable, state estimation techniques should be used to provide the information. The model is identified from the input-output data generated from the batch reactor closed-loop simulations, i.e. with the risk controller on. In this work, the objective function of the optimizer is set to meet the end-batch quality target, which is defined against the concentration of reactant A. In what follows, we present three scenarios to showcase the agility of the proposed hierarchical strategy fitting the purpose for various process dynamics and requirements. Namely: (1) Two-level controller and optimizer integration, (2) Three-level integration with intermediate surrogate model, and (3) Quality control with fixed batch duration.

Scenario 1: Two-Level Controller and Optimizer Integration

Herein, the time step for the optimizer is selected as 20 minutes while forecasting over the next operation. The resulting optimal input and output set points are directly passed to the risk controller, the latter of which has a time step of 5 minutes. The optimizer time step also represents the frequency at which it provides updated set points to the controller. The optimizer tuning parameters and path constraints are provided below in Tables 5 and 6. Scenario 2 will showcase an optimizer set up with significantly longer time step which necessitates the use of intermediate surrogate model, and Scenario 3 will apply a time-varying optimizer with forecast horizon all the way to the end of batch.

Table 5: Scenario 1 – Optimizer tuning parameters

W_1	W_3	p_1	p_3	OH_T	CH_T
1×10^4	1×10^{-6}	2	2	4	3

Table 6: Scenario 1 – Optimizer path constraints

	U^R_{lT}	$C^R_{A,lT}$	$\overline{x}_1, \overline{x}_2, \overline{x}_3, \overline{x}_4$
Min	400	0	$-100, -100, -100, -100$
Max	470	1	$100, \quad 100, \quad 100, \quad 100$

With the controller and optimizer integration, the batch operating trajectories are shown in Figs. 7-10 respectively illustrating the concentration of reactant A, dynamic risk, reactor temperature, and heat transfer coefficient. Three end-point concentrations (i.e. $C_A^{QT} = 0.1$, 0.05, and 0.01 mol/L) are examined to demonstrate the capability of quality target tracking. As shown in Fig. 7, the operating paths under different quality targets are identical until reaching the first quality target ($C_A^{QT} = 0.1$ mol/L). The three quality targets are satisfied within 3, 4, and 7 hours respectively. The varying batch times are a result of the well controlled trade-off between reaction productivity and process risk, as the elevated reactor temperature can accelerate the batch production while posing higher risk. As depicted in Figs. 8 and 9, the controller and optimizer begin with the strategy to take a maximally acceptable risk up to the upper control limit (i.e., 475 K), which strive to boost the reaction productivity for quality considerations. Thus, the reactor is initially heated up as shown by the manipulated variable profile in Fig. 10. However, the utility input switches to cooling at 0.5 hours as the process is forecast to enter the high risk region if heating continues.

Moreover, the predictive behavior of the integrated controller and optimizer also shines through when it approaches the quality target. Using $C_A^{QT} = 0.01$ mol/L as an example, rapid cooling begins at 5 hours when the quality target is about to be met, with the heat transfer coefficient surges to the maximum 5.5×10^4 W/m^{2}K to cease the reaction. Slight Offset is observed, e.g.the process ends at $C_A \approx 0.03$ mol/L for the quality target of 0.01 mol/L. The accuracy of quality control will be remedied later using quality control with fixed batch duration (Scenario 3). Interestingly, if the quality controller is dormant initially and then activated later, a similar heating surge as in Fig. 10 is present at the moment of activation. This further suggests that the long-term optimizer tends to keep the reactor at a relatively higher risk level to meet quality targets in a swift manner, while the controller alone takes more conservative actions prioritizing risk management.

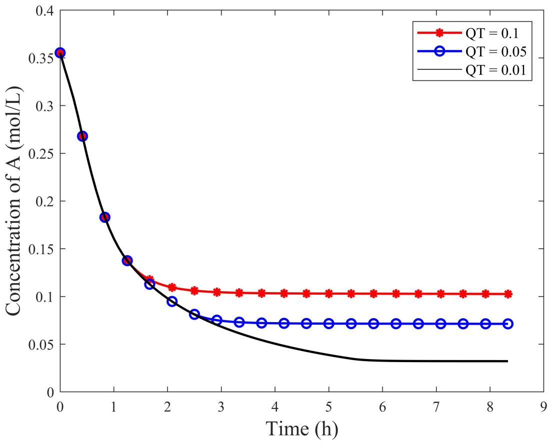

Figure 7: Scenario 1 – End-batch quality control for various quality targets.

Scenario 2: Three-Level Integration with Surrogate Model

In certain instances where the long term and short term time spans are substantially different, issues may arise if: (i) the controller can achieve the set point determined by the optimizer in a short time, and (ii) the optimizer may neglect important short-term dynamics. To test this scenario, the quality and safety optimizer adopts a time step of one hour to prolong the batch operation forecast and enhance long

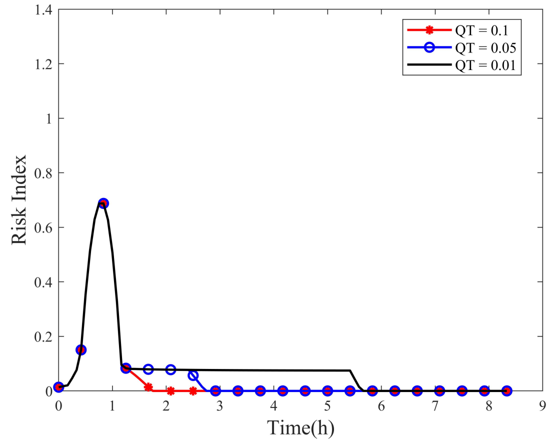

Figure 8: Scenario 1 – Dynamic risk profiles for quality control.

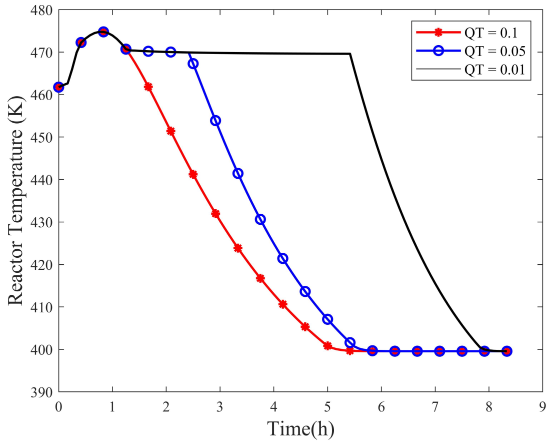

Figure 9: Scenario 1 – Temperature profiles for quality control.

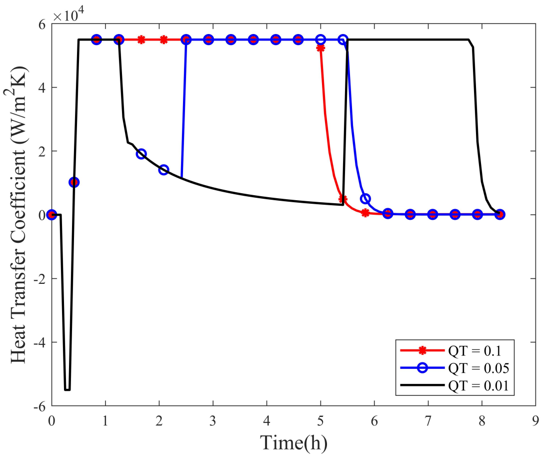

Figure 10: Scenario 1 – Manipulated variable responses for quality control.

term predictions. It is set to forecast 4 hours into the future and provides set point updates every hour to the risk controller. As shown in Fig. 11, if the set points are directly sent from the optimizer to the controller without an intermediate surrogate model, the decision makers are unable to meet the quality target at 0.1 mol/L. This is because the optimizer with $T_s = 1$ hour cannot account for the early reaction dynamics, particularly those occurring during the first hour.

In this context, an intermediate surrogate model is essential to bridge the gap and act as a middle decision maker as per Fig. 2. The surrogate modeling scheme is developed and applied according to Eq. 9 which predicts over 30 minutes and provides updated set points every 10 min. The long-term quality and safety optimizer thus provides updated set points to the surrogate model, the latter of which further computes more reasonable set points at a shorter time span to guide the risk-aware controller. As shown in Fig. 11, the quality target can be met with the aid of surrogate model. The consequence a longer sampling rate is highlighted in Fig. 12 where a higher risk than both Scenario 1 and 3 is attained. The slight offset is comparable to that in Scenario 1. Based on these results, the surrogate modeling technique proves to be successful at translating the long time span operational goals to the short time span risk-aware controller.

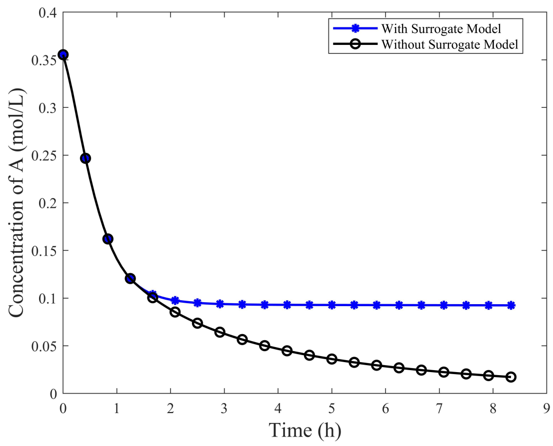

Figure 11: Scenario 2 – Quality control with surrogate modeling

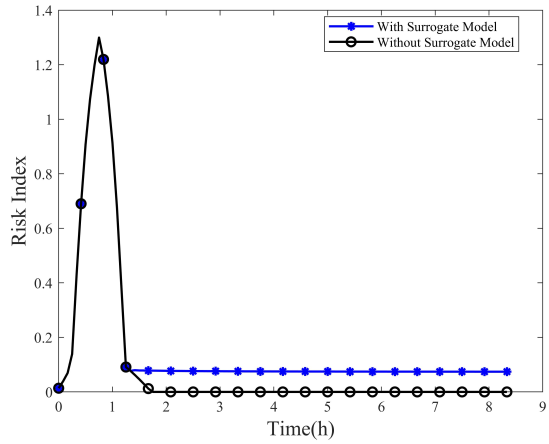

Figure 12: Scenario 2 – Dynamic risk profiles with surrogate modeling

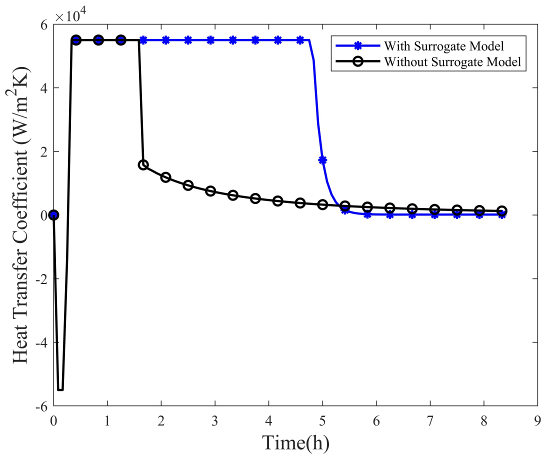

Figure 13: Scenario 2 – Manipulated variable profiles with surrogate modeling

Scenario 3: Quality control with fixed batch duration

The optimizer in the previous scenarios utilize a fixed and rolling output forecast horizon, e.g.1 hour in Scenario 1 or 4 hours in Scenario 2. In this way, the operating strategy is optimized to meet the end-batch quality target as soon as possible while a batch duration is not strictly posed. Hereafter, we consider a fixed total batch duration and require the optimizer to always predict up to the end-point time. This results in a much larger number of optimizer output horizons to be solved using multi-parametric optimization. More importantly, the explicit solutions need to be updated at each time step as the number of output horizons is manipulated to be one less at each successive time step. According to the results of

Scenario 1, the quality targets of 0.1, 0.05, and 0.01 mol/L require 3, 4, and 7 hours respectively. For the quality optimizer with 15-minute time step, 12, 16, and 28 output horizons are respectively required for each quality target at the initial time point. The resulting operating trajectories of this approach are shown in Figs. 14-16. This method is demonstrated to be effective in meeting the quality targets while maintaining safe operations. The offset for $QT = 0.1$ mol/L is comparable to the previous scenarios, while notably less for the quality targets of 0.05 mol/L and 0.01 mol/L. However, the manipulated variable U appears to be sporadicas shown in Fig. 16. This operating strategy also requires more computational time due to the increased and time-varying number of optimizer output horizons. For the largest output horizon ($OH = 28$), the total number of critical regions to be stored for offline mp-MIQP solutions is 6,639. The quality target of 0.01 mol/L takes the longest to compute with a time of 3.25 minutes and the target of 0.1 mol/L takes 0.52 minutes. The computational times in Scenarios 1 and 2 are all within 6 seconds. These studies are carried out on an Alienware m16 with an Intel i9-13900HX CPU and an NVIDIA GeForce RTX 4090 Laptop GPU.

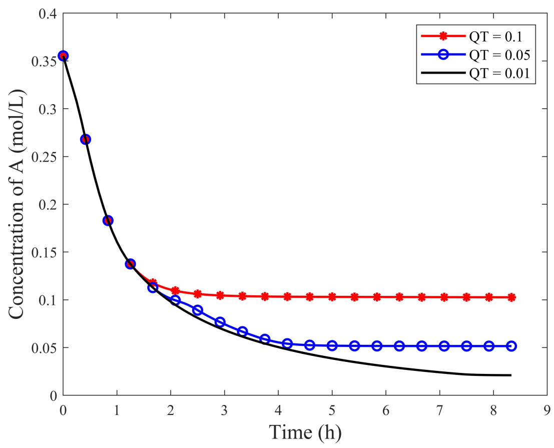

Figure 14: Scenario 3 – Quality control with fixed batch duration

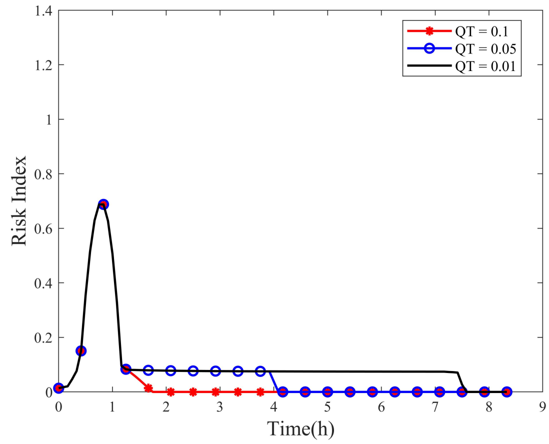

Figure 15: Scenario 3 – Dynamic risk profiles

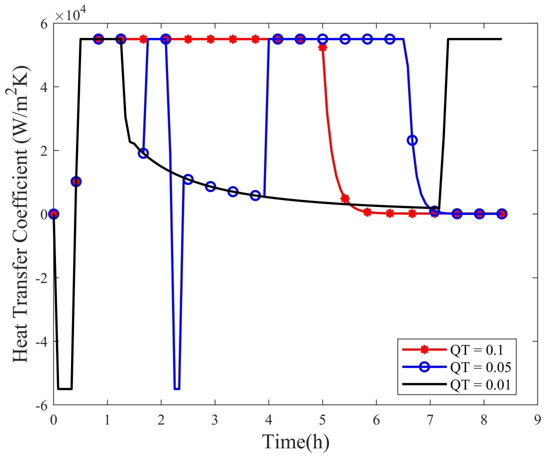

Figure 16: Scenario 3 – Manipulated Variable profiles

4. Conclusions

In this work, we have developed a hierarchical multi-parametric optimization approach for multi-time-scale operational optimization, with application to the integration of model predictive control, end-point batch quality control, and prescriptive risk management. A short-term risk-aware controller is utilized for risk control, set point tracking, and disturbance rejection together with a long-term optimizer to meet batch quality targets and enhance overall operational safety. The methodology is made more robust through the formulation and implementation of an intermediate surrogate model when necessary. The effectiveness and potential of the approach is demonstrated on a safety-critical exothermic batch reactor.

The proposed approach is complementary to economic model predictive control [57, 58] which addresses simultaneous economics and control considerations at every time step. It allows for decomposing the multi-time-scale to a hierarchy of operational optimization problems at the respective characteristic time scales. This can provide more flexibility for problem formulation. In addition to leveraging the long-term optimizer for cost optimization (hours) and the short-term controller for risk control (minutes), the surrogate model creates another intermediate which can be leveraged for, e.g.fault prognosis (20 min to activate alarm in advance).

This work utilizes multi-parametric (mixed-integer) linear/quadratic optimization based on linearized process model. Though the optimization algorithms relieve online computational strain, a desired trait for the long prediction horizons necessary in this work, linearizing process and risk models compromises the accuracy of the system projections in the optimization problem. Linearization in this system is shown to be acceptable as the case studies are validated against the original nonlinear process model. However, in some systemslinearizations may lead to undesirable performance or infeasible actions. Reduced order modeling (ROM) or model order reduction (MOR) techniques offer ways to reduce the computational complexity of high-fidelity models without compromising performance or accuracy. Koopman operator theory is one such technique that provides the capability to fully represent nonlinear dynamics as a globally linear model [59, 60]. Deriving the operator can be quite challenging and real-world implementations often involve approximations of the operator [61]. Recent research using machine learning has found approaches to approximate these operators [62, 63]. Using the Koopman operator method in this system would integrate nicely into the proposed approaches while potentially mitigating any linearization errors made. Additionally, in our prior work [51], we have developed multi-parametric MPC based on a nonlinear machine learning-based process model with a self-adaptive linearization algorithm. This can be readily applied to this work and to enhance the applicability of the proposed approach. It is of the authors' ongoing work to develop robust risk control strategies to address the linearization errors. Additionally, the current approach assumes an accurate online output measurement to estimate the system states, but such accurate measurements may not be always available in practice. In more complex systems, such as pharmaceutical processes, it can be especially challenging to obtain the desired state information. State estimators like the Kalman filter are commonly used in practice but typically rely on the assumption that the uncertainty in the system follows a Gaussian distribution. For these reasons, ongoing work will extend the proposed framework by incorporating Bayesian state estimators to enhance the control optimization performance under generalizable uncertainties.

Acknowledgments

The authors acknowledge financial support from NSF RETRO Project CBET-2312457, NSF F2F Seed Project OIA-2119654, NSF GRFP under Grant No. DGE-1102689, and the Department of Chemical and Biomedical Engineering at West Virginia University.

References

[1] O. Andrés-Martínez, L. A. Ricardez-Sandoval, Integration of planning, scheduling, and control: A review and new perspectives, The Canadian Journal of Chemical Engineering 100 (2022) 2057–2070.

[2] E. N. Pistikopoulos, Y. Tian, Advanced modeling and optimization strategies for process synthesis, Annual Review of Chemical and Biomolecular Engineering 15 (2024).

[3] L. Wu, X. Yin, L. Pan, J. Liu, Distributed economic predictive control of integrated energy systems for enhanced synergy and grid response: A decomposition and cooperation strategy, Applied Energy 349 (2023) 121627.

[4] Y. Bu, C. L. Swartz, C. Wu, A two-level mpc method for the operation of a gas pipeline system under demand variation, Computers & Chemical Engineering 183 (2024) 108597.

[5] Y. Yabuki, T. Nagasawa, J. F. MacGregor, Industrial experiences with product quality control in semi-batch processes, Computers & chemical engineering 26 (2002) 205–212.

[6] G. Caygill, M. Zanfir, A. Gavriilidis, Scalable reactor design for pharmaceuticals and fine chemicals production. 1: Potential scale-up obstacles, Organic process research & development 10 (2006) 539–552.

[7] P. Mhaskar, A. Garg, B. Corbett, Modeling and control of batch processes, Springer, 2015.

[8] S. Russell, D. Robertson, J. Lee, B. Ogunnaike, Model-based quality monitoring of batch and semi-batch processes, Journal of process control 10 (2000) 317–332.

[9] C. Kravaris, R. A. Wright, J. Carrier, Nonlinear controllers for trajectory tracking in batch processes, Computers & chemical engineering 13 (1989) 73–82.

[10] R. Rendall, L. H. Chiang, M. S. Reis, Data-driven methods for batch data analysis–a critical overview and mapping on the complexity scale, Computers & Chemical Engineering 124 (2019) 1–13.

[11] P. Nomikos, J. F. MacGregor, Monitoring batch processes using multiway principal component analysis, AIChE Journal 40 (1994) 1361–1375.

[12] P. Nomikos, J. F. MacGregor, Multi-way partial least squares in monitoring batch processes, Chemometrics and intelligent laboratory systems 30 (1995) 97–108.

[13] S. W. Choi, J. Morris, I.-B. Lee, Dynamic model-based batch process monitoring, Chemical Engineering Science 63 (2008) 622–636.

[14] D. Ghosh, P. Mhaskar, J. F. MacGregor, Hybrid partial least squares models for batch processes: integrating data with process knowledge, Industrial & Engineering Chemistry Research 60 (2021) 9508–9520.

[15] M. Yao, H. Wang, W. Xu, Batch process monitoring based on functional data analysis and support vector data description, Journal of Process Control 24 (2014) 1085–1097.

[16] S. Kay, H. Kay, M. Mowbray, A. Lane, C. Mendoza, P. Martin, D. Zhang, Integrating autoencoder and heteroscedastic noise neural networks for the batch process soft-sensor design, Industrial & Engineering Chemistry Research 61 (2022) 13559–13569.

[17] J. Flores-Cerrillo, J. F. MacGregor, Latent variable mpc for trajectory tracking in batch processes, Journal of process control 15 (2005) 651–663.

[18] S. Aumi, B. Corbett, P. Mhaskar, Model predictive quality control of batch processes, in: 2012 American Control Conference (ACC), IEEE, 2012, pp. 5646–5651.

[19] L. Chang, X. Liu, M. A. Henson, Nonlinear model predictive control of fed-batch fermentations using dynamic flux balance models, Journal of Process Control 42 (2016) 137–149.

[20] S. Lucia, J. A. E. Andersson, H. Brandt, A. Bouaswaig, M. Diehl, S. Engell, Efficient Robust Economic Nonlinear Model Predictive Control of an Industrial Batch Reactor, IFAC Proceedings Volumes 47 (2014) 11093–11098.

[21] M. M. Rashid, P. Mhaskar, C. L. E. Swartz, Handling multi-rate and missing data in variable duration economic model predictive control of batch processes, AIChE Journal 63 (2017) 2705–2718.

[22] E. N. Pistikopoulos, N. A. Diangelakis, R. Oberdieck, Multi-parametric optimization and control, John Wiley & Sons, 2020.

[23] B. Burnak, N. A. Diangelakis, J. Katz, E. N. Pistikopoulos, Integrated process design, scheduling, and control using multiparametric programming, Computers & Chemical Engineering 125 (2019) 164–184.

[24] Y. Tian, I. Pappas, B. Burnak, J. Katz, E. N. Pistikopoulos, Simultaneous design & control of a reactive distillation system–a parametric optimization & control approach, Chemical Engineering Science 230 (2021) 116232.

[25] A. Mesbah, J. Landlust, A. Huesman, H. Kramer, P. Jansens, P. Van den Hof, A model-based control framework for industrial batch crystallization processes, Chemical Engineering Research and Design 88 (2010) 1223–1233.

[26] C. Ji, W. Sun, A review on data-driven process monitoring methods: Characterization and mining of industrial data, Processes 10 (2022) 335.

[27] S. Venkatasubramanian, S. Raja, V. Sumanth, J. N. Dwivedi, J. Sathiaparkavi, S. Modak, M. L. Kejela, et al., Fault diagnosis using data fusion with ensemble deep learning technique in iiot, Mathematical Problems in Engineering 2022 (2022).

[28] V. Venkatasubramanian, R. Rengaswamy, K. Yin, S. N. Kavuri, A review of process fault detection and diagnosis: Part i: Quantitative model-based methods, Computers & chemical engineering 27 (2003) 293–311.

[29] A. A. Amin, K. M. Hasan, A review of fault tolerant control systems: advancements and applications, Measurement 143 (2019) 58–68.

[30] M. A. Djeziri, S. Benmoussa, M. E. Benbouzid, Data-driven approach augmented in simulation for robust fault prognosis, Engineering Applications of Artificial Intelligence 86 (2019) 154–164.

[31] M. T. Amin, R. Arunthavanathan, M. Alauddin, F. Khan, State-of-the-art in process safety and digital system, in: Methods in Chemical Process Safety, volume 6, Elsevier, 2022, pp. 25–59.

[32] F. Crawley, B. Tyler, HAZOP: Guide to best practice, Elsevier, 2015.

[33] C. H. Lim, S. Lim, B. S. How, W. P. Q. Ng, S. L. Ngan, W. D. Leong, H. L. Lam, A review of industry 4.0 revolution potential in a sustainable and renewable palm oil industry: Hazop approach, Renewable and Sustainable Energy Reviews 135 (2021) 110223.

[34] Center for Chemical Process Safety (CCPS), Guidelines for risk based process safety, John Wiley & Sons, 2010.

[35] F. Khan, P. Amyotte, S. Adedigba, Process safety concerns in process system digitalization, Education for Chemical Engineers 34 (2021) 33–46.

[36] T. M. Ahooyi, M. Soroush, J. E. Arbogast, W. D. Seider, U. G. Oktem, Model-predictive safety system for proactive detection of operation hazards, AIChE Journal 62 (2016) 2024–2042.

[37] F. Albalawi, H. Durand, P. D. Christofides, Process operational safety via model predictive control: Recent results and future research directions, Computers & Chemical Engineering 114 (2018) 171–190.

[38] J. A. Venkidasalapathy, C. Kravaris, Safety-centered process control design based on dynamic safe set, Journal of Loss Prevention in the Process Industries 65 (2020) 104126.

[39] Z. Wu, P. D. Christofides, Process operational safety and cybersecurity, Springer, 2021.

[40] Y. A. Kadakia, A. Suryavanshi, A. Alnajdi, F. Abdullah, P. D. Christofides, Integrating machine learning detection and encrypted control for enhanced cybersecurity of nonlinear processes, Computers & Chemical Engineering 180 (2024) 108498.

[41] A. Meel, W. D. Seider, Plant-specific dynamic failure assessment using bayesian theory, Chemical engineering science 61 (2006) 7036–7056.

[42] V. Villa, N. Paltrinieri, F. Khan, V. Cozzani, Towards dynamic risk analysis: A review of the risk assessment approach and its limitations in the chemical process industry, Safety science 89 (2016) 77–93.

[43] A. Raveendran, V. Renjith, G. Madhu, A comprehensive review on dynamic risk analysis methodologies, Journal of Loss Prevention in the Process Industries 76 (2022) 104734.

[44] B. Bhadriraju, J. S.-I. Kwon, F. Khan, Risk-based fault prediction of chemical processes using operable adaptive sparse identification of systems (oasis), Computers & Chemical Engineering 152 (2021) 107378.

[45] H. Bao, F. Khan, T. Iqbal, Y. Chang, Risk-based fault diagnosis and safety management for process systems, Process Safety Progress 30 (2011) 6–17.

[46] M. Ali, X. Cai, F. I. Khan, E. N. Pistikopoulos, Y. Tian, Dynamic risk-based process design and operational optimization via multi-parametric programming, Digital Chemical Engineering 7 (2023) 100096.

[47] E. N. Pistikopoulos, Y. Tian, Synthesis and Operability Strategies for Computer-Aided Modular Process Intensification, Elsevier, 2022.

[48] A. P. Ortiz-Espinoza, A. Jiménez-Gutiérrez, M. M. El-Halwagi, N. K. Kazantzis, V. Kazantzi, Comparison of safety indexes for chemical processes under uncertainty, Process Safety and Environmental Protection 148 (2021) 225–236.

[49] C. Kravaris, I. K. Kookos, Understanding Process Dynamics and Control, Cambridge University Press, 2021.

[50] P. Rivotti, R. S. Lambert, E. N. Pistikopoulos, Combined model approximation techniques and multiparametric programming for explicit nonlinear model predictive control, Computers & Chemical Engineering 42 (2012) 277–287.

[51] W. Wang, Y. Wang, Y. Tian, Z. Wu, Explicit machine learning-based model predictive control of nonlinear processes via multi-parametric programming, Computers & Chemical Engineering (2024) 108689.

[52] W. Tang, P. Daoutidis, Data-driven control: Overview and perspectives, in: 2022 American Control Conference (ACC), IEEE, 2022, pp. 1048–1064.

[53] A. Braniff, Y. Tian, Dynamic risk-based model predictive quality control with online model updating, in: 2024 American Control Conference (ACC), IEEE, 2024.

[54] Chemical Safety Board, T2 laboratories inc. reactive chemical explosion, www.csb.gov/t2-laboratories-inc-reactive-chemical-explosion (2007).

[55] K. Burn, L. Maerte, C. Cox, A Matlab Toolbox for Teaching Modern System Identification Methods for Industrial Process Control, International Journal of Mechanical Engineering Education 38 (2010) 352–364. Publisher: SAGE Publications Ltd STM.

[56] MATLAB and Statistical Toolbox 2021b, 2021. The MathWorks Inc., Natick, Massachusetts.

[57] L. MacKinnon, C. L. E. Swartz, Robust Multi-Scenario Dynamic Real-Time Optimization with Embedded Closed-Loop Model Predictive Control, IFAC-PapersOnLine 54 (2021) 481–486.

[58] M. Ellis, P. D. Christofides, Real-time economic model predictive control of nonlinear process systems, AIChE Journal 61 (2015) 555–571.

[59] A. Narasingam, J. S.-I. Kwon, Koopman Lyapunov-based model predictive control of nonlinear chemical process systems, AIChE Journal 65 (2019) e16743.

[60] S. H. Son, H.-K. Choi, J. S.-I. Kwon, Application of offset-free Koopman-based model predictive control to a batch pulp digester, AIChE Journal 67 (2021) e17301.

[61] P. Bevanda, S. Sosnowski, S. Hirche, Koopman operator dynamical models: Learning, analysis and control, Annual Reviews in Control 52 (2021) 197–212.

[62] M. Han, Z. Li, X. Yin, X. Yin, Robust Learning and Control of Time-Delay Nonlinear Systems With Deep Recurrent Koopman Operators, IEEE Transactions on Industrial Informatics 20 (2024) 4675–4684. Conference Name: IEEE Transactions on Industrial Informatics.

[63] X. Yin, Y. Qin, J. Liu, B. Huang, Data-driven moving horizon state estimation of nonlinear processes using Koopman operator, Chemical Engineering Research and Design 200 (2023) 481–492.